CrossMark

Changes induced in the luminescent emission of Eu³⁺ by different crystal nature: An analysis by group theory

J. Guzmán Mendoza[a], E. Garfias García[b], J.C. Guzmán Olguín[a], E. Montes[a,*], G. Torres Jasso[a], M. García-Hipólito[c], C. Falcony-Guajardo[d]

[a] Centro de Investigación en Ciencia Aplicada y Tecnología Avanzada del Instituto Politécnico Nacional, Unidad Legaria, Calzada Legaria 694. Col. Irrigación, C.P. 11500 Cd. de México, Mexico
[b] Dpto. de Materiales, DCBI, Universidad Autónoma Metropolitana, Av. San Pablo 180, Col. Reynosa Tamaulipas, 02200 Ciudad de México, Mexico
[c] Instituto de Investigaciones en Materiales, Universidad Nacional Autónoma de México, Circuito Exterior, Ciudad Universitaria, Coyoacán, 04510 Cd de México, Mexico
[d] Centro de Investigación y de Estudios Avanzados del Instituto Politécnico Nacional, A.P. 14-740, Cd. de México 07360, Mexico

ARTICLE INFO

ABSTRACT

The effects of the crystal nature on the luminescent emission of Eu^{3+} ion in Y_2O_3, HfO_2 and ZrO_2 oxides, synthesized by the hydrothermal route are reported. The luminescent spectra at room temperature, showed the peaks associated with the characteristic transitions of Eu^{3+} ion, observing significant changes in the electric dipole transition $^5D_0 \rightarrow {}^7F_1$ ($D° \rightarrow D^1$), in each of the different crystals; the analysis by group theory allowed us to offer an explanation of the differences presented in the emission spectra in the different crystals.

1. Introduction

The increasing interest in nanostructured materials with applications in photonics and optoelectronics has led the scientific community to turn their attention to materials doped with rare earth elements, considered the greatest activators of luminescence [1–3]. From the point of view of basic physics, it is of fundamental importance to understand the luminescent behavior of rare earth ions when they are introduced in nanostructured structures and how their emission spectra change with the environment where they are immersed. Several reports have been made on different types of materials that have been doped with rare earth ions for luminescent applications, ranging from sulfides, fluorides, hafnates, vanadates, etc. [4–6]. Among the materials used as host luminescent materials, are the metallic oxides, which are very versatile materials that have a great number of applications, between which we can mention waveguides, hard coatings, gas sensors, dosimeters, etc. [7–9]. In particular, metal oxides have been investigated in luminescent applications as host lattice to harbor rare earth ions due to their thermal and chemical stability, high phononic frequency and wide bandgap, which makes them good candidates for use in flat panels, optical amplifiers, in up conversion processes and systems to generate images in medicine [10–12]. There are different techniques to synthesize metal oxide powder, among which we can mention the methods of sol-gel, co-precipitation, reactions in solid state, etc. [13–15], however the hydrothermal synthesis process is a simple technique of low energy

consumption that allows us to obtain nanostructured materials and that, when using chlorides as precursors and sodium hydroxide as a pH modifier, does not generate a negative impact on the environment, since sodium chloride is obtained as a result of the reaction, in addition to the reaction being carried out in a closed system. Since rare earth elements are characterized by an incompletely filled 4f shell, the 4f orbitals are shielded from the surrounding by the $5s^2$ and $5p^2$ orbitals, they are little influenced by the crystalline field of the host, however, although this small influence can lead to modifications with important consequences in their luminescent emission spectra, depending where they are housed.

Using group theory it is possible to understand some of the optical properties of optically active centers such as trivalent Europium (Eu^{3+}); by analyzing the symmetry properties of the optically active center (ie the ion and its local environment), this theory allows us to determine the number of energy levels of a particular active center, to label these electronic energy levels by means of irreducible representations, determine its degeneracy, establish selection rules for optical transitions and determine their polarization. The Eu^{3+} ion is commonly used to develop devices with a red emission, because their electronic transitions are most likely to occur between 550 and 700 nm. Due to its electronic structure, these transitions are not affected in their position by any type of field generated by their environment, but the probability of occurrence yes, as well as the number of degenerations; If the ion within the crystal occupies a site with inversion symmetry, then

any transition of an electric dipole type is forbidden, leaving only the magnetic dipole type ($\Delta J = 0, \pm 1$, but from $J = 0$ to $J = 0$ it is forbidden). If there is no inversion symmetry at the site of the ion, the uneven crystalline field generated by the environment on the ion, mixes the states with opposite parities within the configurational levels $4f^n$ and the dipole electric transitions appear. This effect hypersensitizes some transitions ($\Delta J = 0, \pm 2$, but from $J = 0$ to $J = 0$ is prohibited), which appear predominantly in the spectrum. Few studies have been carried out on the effect of crystal structure on emission spectra of rare earth ions; To establish this phenomenon, in this work we carry out a study on the induced changes in the luminescent emission spectrum of the Eu^{3+} ion when it is introduced in three different metal oxides hosts zirconium oxide (ZrO_2), hafnium oxide (HfO_2) and yttrium oxide (Y_2O_3); Interpreting these modifications in emission spectra to the light of group theory.

2. Experimental procedure

The synthesis of the ZrO_2, HfO_2 and Y_2O_3 doped with Eu^{3+} (3 at%) were synthesized by the hydrothermal route. $ZrOCl_2 \cdot 8H_2O$ (Fluka 99.0%), hafnium chloride $HfCl_4$ (Alfa Aesar 99.9%) and yttrium chloride YCl_2 (Aldrich 99.0%) were used as precursors for the different oxides. $EuCl_3 \cdot 6H_2O$ (Aldrich 99.9%) was used as the precursor for the impurity and a solution of sodium hydroxide (NaOH) (Aldrich 97%) was used to adjust the acidity of the solutions; using deionized water as solvent in all cases. The synthesis of the ZrO_2 was carried out from a 0.02 M aqueous solution of $ZrOCl_2$; 4.3 mg of $EuCl_3$ (3 at% Eu/Zr in solution) was added to the stock solution. To adjust the acidity of the solution to pH = 11; a 2 M solution of NaOH was used by adding dropwise. In the case of HfO_2, also a 0.02 M stock solution of $HfCl_4$ was used, doped with 4.3 mg of $EuCl_3$ (3% of Eu/Hf in solution); the acidity of the solution was adjusting to pH = 12 with a 2 M solution of NaOH.

Yttrium oxide was synthesized from a 0.04 M stock solution of yttrium chloride and 8.6 mg of europium chloride was added to the stock solution. The acidity of the solution was adjusted by adding a 0.02 M solution of NaOH dropwise to pH of 7. In this case the formation of a white precipitate from an acidity of pH = 4 was observed due to complex formation $M_x(OH)_y$ (M = Zr, Hf, Y, Eu). In all cases, the suspensions obtained were maintained under constant magnetic stirring during the procedure. After completion of the preparation of the solutions, all of them were subjected to hydrothermal treatment for a reaction time of 90 min at a temperature of 200 °C, under autogenous pressure. The powder obtained was washed successively with deionized water and then dried at 80 °C for 5 h.

3. Results and analysis

The structural characterization was carried out by X-ray diffraction (XRD) in a Bruker D8-Advance diffractometer, using a wavelength of $\lambda = 1.5406$ Å, corresponding to the Kα line of emission of the Cu, with steps of 0.05° and 0.05 s per step. The results obtained are shown in Fig. 1, in which it can be seen the different crystalline structures of the synthesized materials; The Y_2O_3 show a body centered cubic structure with spatial group $Ia\bar{3}$ corresponding to the diffraction chart ICDD-00-034-1036. The HfO_2 presents a monoclinic structure with space group $P2_1/c$, corresponding to the diffraction chart ICDD-00-065-1142. Finally the ZrO_2 presents a mixture of two phases, the monoclinic phase with space group $P2_1/a$ and diffraction card PDF-72-1669, combined with the tetragonal phase with space group $P4_2/nmc$ corresponding to the diffraction card ICSD-066783. These results will allow us to carry out the study of the effect that the crystalline structure has on Eu^{3+} ion in the luminescent emission.

Transmission electron microscopy (TEM) characterization was performed on a JEOL JEM 1200 EX microscope with. Fig. 2 shows the transmission micrographs of the HfO_2 and ZrO_2 samples; the angles between the faces of the particles correspond to those of the monoclinic
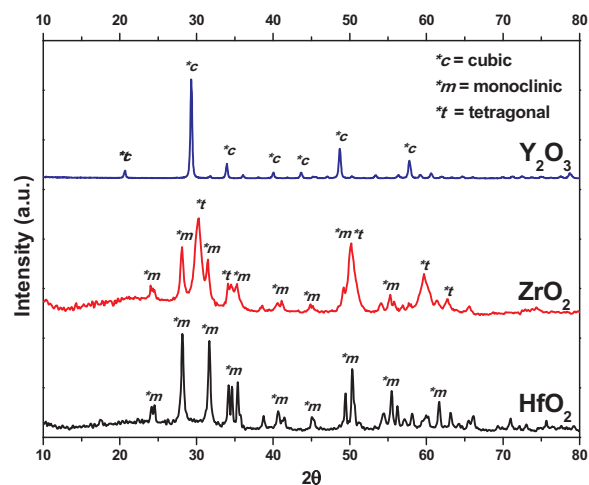

Fig. 1. X-ray diffraction patterns of the different synthesized samples.

structure found in the XRD analysis. For the characterization morphological was used a high resolution scanning electron microscope (HRSEM), Zeiss brand, model SUPRA 55 VP with Gemini column and field emission gun, using the secondary electron detector. Fig. 3 shows the high resolution scanning micrographs of ZrO_2, HfO_2 and Y_2O_3. In the first two, the microstructure of zirconium oxide can be observed. Fig. 3(a) shows particles of 100 nm in oval form, corresponding to the monoclinic structural, while Fig. 3(b) shows particles in the form of deformed cubes greater than 200 nm; This morphology corresponds to the tetragonal structure; These results are in agreement with the results obtained by XRD, where diffraction peaks associated to both phases appear. Fig. 3(c) show the HRSEM micrograph of the HfO_2, where oval-shaped particles of about 100 nm can be seen; The shape of the particles is the result of the crystalline growth of the material; In the same manner as in zirconium oxide, this microstructure corresponds to the monoclinic structure determined by X-ray diffraction. Finally, Fig. 3(d) corresponds to the HRSEM micrograph of Y_2O_3, in which particles with sizes greater than 200 nm can be observed, which correspond well to the narrow peaks obtained by X-ray diffraction.

The photoluminescent characterization was performed on a Perkin-Elmer LS50B spectrometer. In all cases, the emission spectra were obtained at room temperature using an excitation wavelength of 395 nm. Fig. 4 shows the photoluminescent emission spectrum of the ZrO_2:Eu^{3+} (3 at%), where the peaks associated with the characteristic transitions of Eu^{3+} ion can be observed. The most intense band appears at 608 nm, corresponding to the $^5D_0 \rightarrow {}^7F_2$ transition, which generates the red color, characteristic of Eu^{3+} ion. The intense band appearing at 593 nm, corresponding to the $^5D_0 \rightarrow {}^7F_1$ transition, with emission in yellow; Also appear other characteristic emissions of the Eu^{3+} ion centered on 580, 653 and 714 nm. However, the peaks corresponding to transitions $^7F_1$ and $^7F_2$, do not present a remarkable difference in height, indicating that both transitions are almost as likely to occur and appear very narrow, indicating a lower intensity in the vibronic coupling between the ion and the matrix (Fig. 5).

Using group theory, we can analyze the emission spectrum of ZrO_2:Eu^{3+} (3 at%), which is shown in Fig. 4. The character table of point group D_{4h}, corresponding to the structure monoclinic of ZrO_2, is shows in the Table 1 [16], it show the irreducible representations associated with the components of the electric dipole, A_{2u} (z) and E_u (x, y). Representations are named according to a set of conventions: A, when the rotation around the principal axis is symmetric; B, when the rotation about the main axis is asymmetric; E and T are two-fold and triple-degenerate representations, respectively. From the previous character table, we construct the D^J representations ($J = 0,1,2,3$) in the group D_{4h}, and we decompose them into irreducible representations [17]. Fig. 6 shows the dipole electric transitions of the Eu^{3+} in an